Mesoscopic Structures of Nanocrystals: Collective Magnetic Properties Due to the Alignment of Nanocrystals

Y. Lalatonne,[†] L. Motte,[†] V. Russier,[†] A. T. Ngo,[†] P. Bonville,[‡] and M. P. Pileni*[,†]

Laboratoire des Matériaux Mésoscopiques et Nanométriques U.M.R. 7070, Université Pierre et Marie Curie, BP 52, 4 place Jussieu, 75005 Paris, France, and Centre d'Etudes de Saclay, Commissariat à l'Energie Atomique, DRECAM/SPEC, 91191 Gif-sur-Yvette cedex, France

Received: June 11, 2003

Maghemite nanocrystals, deposited by slow evaporation on HOPG (highly oriented pyrolytic graphite) substrate, form mesoscopic structures which strongly depend on the nanocrystal coating. When the coating consists of citrate ions and octanoic acid, tubelike structures are formed when the deposition process takes place under an applied magnetic field. Conversely, dense films are formed when the nanocrystals are coated with propanoic acid and dodecanoic acid. The magnetic behaviors markedly differ with the organization of nanocrystals and are attributed to the change in the anisotropy of the organized structures. Nanocrystals organized in tubes behave as nanowires.

I. Introduction

Magnetic nanocrystals have generated much interest because of their large domain of applications, especially for their relevance in high-density magnetic recording devices.[1] For nanowires, it has been well established that the shape anisotropy induces changes in magnetic properties compared to those of the unstructured material, the hysteresis curve being more rectangular (respectively smoother) when the field is applied parallel (respectively perpendicular) to the wires' axis. The reduced remanence and coercivity values vary depending on the length[2] and the diameter of the wires[3] as well as the packing density.[4]

In the past few years, we developed a new technique to produce mesoscopic structures.[5,6] We showed that the magnetic properties drastically change with the strength of the field applied during the deposition. This was attributed to a partial orientation of the easy magnetic axis of each individual particle.

In the present paper, it is demonstrated that the nanocrystal coating plays an important role in determining the mesoscopic structures and the magnetic properties. When nanocrystals are arranged in tubes, they behave as nanowires.

II. Experimental Section

II.1. Apparatus. A JEOL(100 kV) model JEM 100 CX II and a JEOL model JSM-840A were used for transmission electron microscope (TEM) and scanning electron microscope (SEM) experiments, respectively.

Hysteresis loops at 3 K were measured with a commercial SQUID (superconducting quantum interference device) magnetometer with fields up to 5 T. The ^{57}Fe Mössbauer absorption spectra were recorded at 4.2 K in zero magnetic field, using a ^{57}Co:Rh γ-ray source mounted on an electromagnetic drive with a triangular velocity signal.

II.2. Synthesis and Characterization of Maghemite Nanocrystals Differing by Their Coating. The γ-Fe_2O_3 nanocrystals used in this study and the obtained mesoscopic structures are described in detail elsewhere in a separate publication[7] (see also the Appendix).

The maghemite nanocrystals characterized by the same average size (10 nm) and differing coatings (citrate ions ($C_6O_7H_5^{3-}$), propanoic (C_2H_5COOH), octanoic ($C_7H_{15}COOH$), and dodecanoic ($C_{11}H_{23}COOH$) acids) are produced. Nanocrystals coated with citrate ions and propanoic acid are solubilized in aqueous solution, whereas with octanoic and dodecanoic acid, the solvent is cyclohexane. For simplicity, in the following we will label the nanocrystals according to their coating as follows: CIT (citrate ions), PR (propanoic acid), OC (octanoic acid), and DO (dodecanoic acid).

II.3. Nanocrystals Deposition on a Substrate in the Presence or Absence of a Magnetic Field. The nanocrystals are deposited on an HOPG (highly oriented pyrolytic graphite) substrate by evaporation of a ferrofluid solution. During this process, a magnetic field is or is not applied parallel to the substrate plane.

To obtain quantitatively comparable measurements, it is necessary to deposit the same amount of nanocrystals on the substrate. Hence, the deposition procedure differs according to the coating.

(i) With citrate ions or propanoic acid as the passivating agents (hydrophilic magnetic fluid), the dewetting occurs when a drop is deposited on the substrate. The drop remains on the substrate during the evaporation process. The SEM patterns are obtained when 7 times 10 μL of solution containing 1.1×10^{-2} mol L^{-1} of nanocrystals is deposited on the HOPG substrate.

(ii) With the octanoic or dodecanoic acids as coating agents, the solution wets the substrate. The substrate is then dipped into the solution, and evaporation takes place in a saturated atmosphere in order to increase the evaporation time to 8 h. During this process, the nanocrystals are attracted toward the magnet poles and stick to the glass box. This induces a loss of particles which do not deposit onto the substrate. The amount of material deposited is deduced after evaporation by dispersing the particles remaining in the box with the original solvent and

[†] Université Pierre et Marie Curie.
[‡] Commissariat à l'Energie Atomique.

10.1021/jp035665c CCC: $27.50
Published on Web 01/09/2004

TABLE 1: Variation of Reduced Remanence and Coercivity at 3 K for Isolated Particles Dispersed in Polymer and Deposited with or without a Magnetic Field of 0.59 T during Evaporation[a]

matrix:	PVA	PMMA	HOPG							
sample:	CIT_0	DO_0	CIT_0	$CIT_{0.01}(\|\|)$	$CIT_{0.01}(\perp)$	$CIT_{0.59}(\|\|)$	$CIT_{0.59}(\perp)$	DO_0	$DO_{0.59}(\|\|)$	$DO_{0.59}(\perp)$
M_r/M_s:	0.30	0.30	0.42	0.45	0.37	0.52	0.31	0.42	0.42	0.41
H_c (Oe):	360	370	420	440	390	480	390	420	420	420

[a] For the oriented deposits, the measuring field is applied parallel to the substrate and is either (||) along the direction or ($\perp$) perpendicular to the aligned particles.

measuring the optical density of the remaining solution. The SEM patterns are obtained after the HOPG substrate was deposited into 200 μL containing 1.1×10^{-1} mol L^{-1} of nanocrystals.

By use of the procedures described above, 0.15 mg of 10-nm γ-Fe_2O_3 nanocrystals, differing by their coatings, are deposited on the HOPG substrate with the formation of thick films. The thickness of the sample varies from 3 μm in the center of the sample to 10 μm in its border. This inhomogeneity in the film thickness does not depend on the coating of the nanocrystals used.

For samples deposited in the presence of a magnetic field, the value of the applied field, *x*, during the deposition process is given in the subscript of the name of the sample: CIT_x, PR_x, OC_x, and DO_x.

II.4. Samples for Magnetic Measurements. We first recorded magnetization curves of nanocrystals without interactions, by dispersing a 0.5% weight fraction of nanoparticles dispersed in a nonmagnetic matrix. Because of the difference in solubility between CIT and DO nanocrystals, CIT is dispersed in an aqueous solution of poly(vinyl alcohol), PVA, (1 g/10 cm^3) whereas DO is solubilized in chloroform containing poly (methyl methacrylate), PMMA, (2 g/10 cm^3). The solutions are dried in air yielding rigid pellets.

The magnetic properties are recorded at 3 K using a SQUID. We find that, whatever the coating is, the reduced remanence and the coercive field are 0.30 and 360 $\pm$ 10 Oe, respectively (Table 1). This means that, independent of the coating agent, our passivated maghemite nanocrystals present equivalent individual magnetic properties. This confirms previously published data[8] which showed that the technique developed to produce ferrite nanocrystals allows a change of the coating without any change in the magnetic properties of the nanocrystals. In the present maghemite samples, the reduced remanence value is lower than that calculated for randomly distributed single domain particles either with uniaxial anisotropy ($M_r/M_s = 0.5$)[9] or with cubic anisotropy ($M_r/M_s = 0.8$).[10] Furthermore, as it has been demonstrated by ferromagnetic resonance (FMR) experiments[11] that nanosized particles of γ-Fe_2O_3 possess a positive uniaxial anisotropy, then it is also reasonable to conclude that our γ-Fe_2O_3 nanocrystals are characterized by a uniaxial anisotropy. When the magnetic properties of nanocrystals deposited on HOPG substrate are recorded, the measuring field is always parallel to the substrate plane and its orientation can be chosen in this plane. For nanocrystals forming a dense film, the magnetization curves are the same whatever the field direction in the plane. Conversely, when nanocrystals are organized in tubes, a marked anisotropy of the magnetization is observed. In this case, we define two axes: the *x* axis, parallel to the tube axis made of the nanocrystals, and the *y* axis, perpendicular to it. For simplicity, the orientations of the measuring magnetic field are denoted as (||) and ($\perp$), when the field is along *x* or *y* axis, respectively.

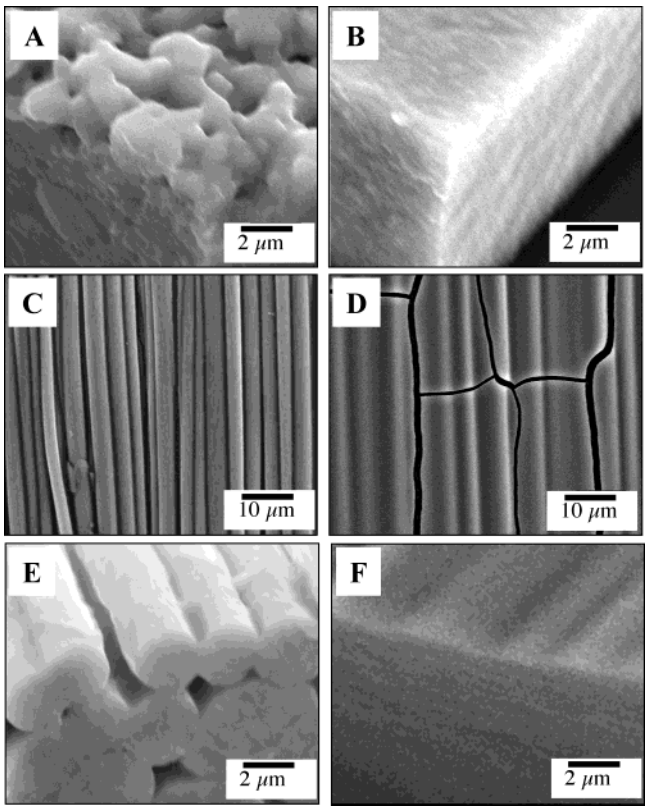

Figure 1. SEM images obtained at various magnifications for maghemite nanocrystals evaporated in the absence and presence of a magnetic field, and with different coatings: CIT_0 nanocrystals (A), DO_0 nanocrystals (B), $CIT_{0.59}$ nanocrystals (C,E), or $DO_{0.59}$ nanocrystals (D,F).

III. Results and Discussion

During the deposition process on the HOPG substrate, a magnetic field can be applied with a strength (as an index to the sample name) varying from 0.01 to 0.59 T.

With no applied magnetic field, the SEM image obtained with CIT_0 nanocrystals (Figure 1A) markedly differs from that obtained with DO_0 (Figure 1B): With CIT_0, the surface is very rough. The film is made of spherical, highly compact agglomerations, with an average diameter of 1.5 $\pm$ 1 μm (Figure 1A). With DO_0, the SEM pattern shows a very flat surface and a high compacity of the film (Figure 1B).

In an applied magnetic field during evaporation, for $CIT_{0.59}$ nanocrystals, we observe the formation of long cylinders with a very regular structure (Figure 1C). By tilting the sample, it is seen that (Figure 1E) the structure corresponds to superimposed tubes with an average diameter of 3 $\pm$ 1 μm. Conversely, with $DO_{0.59}$ nanocrystals, stripes are observed (Figure 1D) on a large scale with a highly dense and undulated structure (Figure 1F).

The magnetization saturation of these nanocrystals deposited on the substrate is reached at 3 T. But the shape of the magnetization curves markedly depends on the type of meso-

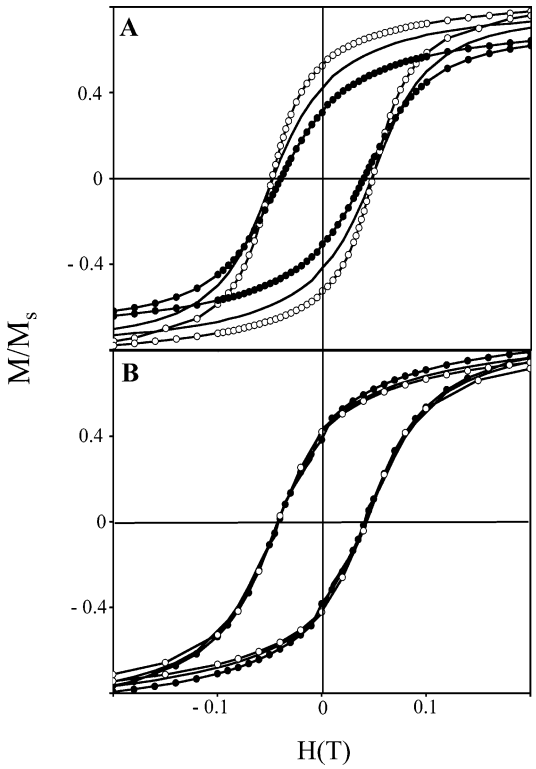

Figure 2. Magnetization curves at 3 K recorded for nanocrystals with either no field (solid line) or a 0.59 T field applied during the deposition process, the measuring field being along the *x* (○) or *y* (●) direction: (A) CIT nanocrystals, (B) DO nanocrystals.

scopic structure (Figure 1), on the coating agent, and on the orientation of the measuring field.

III.1. Shape of the Magnetization Curves With No Magnetic Field. Table 1 shows the same coercive field and reduced remanence for CIT_0 and DO_0. These values are higher than those obtained when the nanocrystals are isolated and dispersed in a polymer indicating an increase in the magnetic interactions when nanocrystals form a thick film.[13]

III.2. Shape of the Magnetization Curves With an Applied Magnetic Field. The hysteresis loop of $CIT_{0.59}$ (||) is squarer than that obtained for CIT_0 and the hysteresis loop of CIT_0 is enclosed inside that of $CIT_{0.59}$ (|| and ⊥). The hysteresis loop of $CIT_{0.59}$ (⊥) is smoother and the coercive field decreases compared to that of CIT_0 (Figure 2A). Conversely, the magnetic behaviors remain the same with DO_o, $DO_{0.59}$(||) ,and $DO_{0.59}$(⊥) (Figure 2B). The influence of the coating on the magnetic properties of nanocrystals deposited under a magnetic field can be attributed to two processes: either the easy magnetic axes have a preferential orientation for one coating and not for the other, or the difference stems from the presence of the specific mesoscopic tubelike structure for the CIT nanocrystals.

III.2.a. Orientation of the Easy Magnetic Axes. During the deposition process, each nanocrystal subjected to a magnetic field rotates inducing an alignment of the easy axis along the direction of the field. Stoner and Wohlfarth[9] find a dependence of the magnetization curve on the angle between the applied field and the easy axis. In the present experiments, 10-nm γ-Fe_2O_3 nanocrystals are spherical and characterized by a uniaxial anisotropy. At room temperature, the ratio of the Zeeman energy, μH, to the thermal energy, k_BT, is equal to 30 (with $H = 0.59$ T). This indicates that the magnetic moment of the particle could be aligned along the magnetic field direction. Moreover, a preferential orientation of the easy axes in the applied magnetic field direction depends on the ratio of the anisotropy energy to the thermal energy, KV/k_BT. Consequently, the anisotropy energy KV (with $K = 6 \times 10^5$ erg cm^{-3}) is 10 times greater than the thermal energy. This clearly indicates that from an energetic viewpoint, nanocrystals should be able to rotate on themselves so that their magnetic moments, pinned along the easy axes, are preferentially aligned with the field.

III.2.b. Influence of the Mesoscopic Structure. Application of a magnetic field during the deposition process induces the formation of well-defined cylinders, which are absent in the mesostructure for DO nanocrystals (Figure 1D,F). Then dipolar interaction effects could be important for the well-ordered structures of CIT nanocrystals.

To discriminate between these two possible origins of the influence of the structuring field on the magnetization curves, ^{57}Fe Mössbauer absorption experiments were performed at 4.2 K, in zero magnetic field, on samples CIT_0, $CIT_{0.59}$, and $DO_{0.59}$, respectively, in order to check whether there exists a preferential orientation of the magnetic moments. For these experiments, 1 mg of nanocrystals is deposited on HOPG, resulting in structures similar to those described in Figure 1. The absorbers were made of the substrate with the deposited nanocrystals, the substrate plane being perpendicular to the γ-ray direction of propagation. For $^{57}Fe^{3+}$, the hyperfine field is antiparallel to the magnetic moment, and in a magnetically ordered powder sample, the direction of the hyperfine field is at random with respect to the laboratory axis consisting of the γ-ray direction. In this case, the intensities of the six lines of the magnetic hyperfine spectrum are in the ratio 3:2:1:1:2:3. If the Fe^{3+} magnetic moments in the entire sample (and thus the hyperfine fields in the whole sample) have a single orientation β with respect to the γ-ray direction of propagation, the intensities of the six hyperfine lines have the following angular dependence:

$$A_{1,6} = 3(1 + \cos^2 \beta)$$
$$A_{2,5} = 4 \sin^2 \beta \qquad (1)$$
$$A_{3,4} = 1 + \cos^2 \beta$$

where $A_{i,j}$ is the intensity of line i or j. It is convenient to use the ratio $r = A_{2,5}/A_{3,4}$ to characterize the degree of alignment or texture of the magnetic moments. If all the Fe moments lie in a plane perpendicular to the γ-ray direction ($\beta = 90°$), the intensities of the six lines are in the ratio 3:4:1:1:4:3. The ratio r is 4, whereas it is 2 for a random orientation of the moments. For partial orientation, intermediate between a random distribution and full orientation perpendicular to the γ-ray direction, the ratio r takes a value between 2 and 4.

Mössbauer spectra are recorded at 4.2 K on absorbers made of the substrate with deposited nanocrystals. The substrate plane is therefore perpendicular to the γ-ray direction. Figure 3 shows the spectra obtained with CIT_0 dispersed in PVA (Figure 3A), with $CIT_{0.59}$ (Figure 3B), and with $DO_{0.59}$ (Figure 3C). The spectra, shown in Figure 3, are quasi-identical with the six lines of a magnetic hyperfine pattern. Note a small asymmetry characteristic of the γ-Fe_2O_3nanocrystals, due to the presence of two Fe^{3+} sites with slightly different hyperfine parameters. The intensity ratio is 2 for CIT_0 in PVA and $DO_{0.59}$, whereas it is 2.15 for $CIT_{0.59}$. Hence, for $DO_{0.59}$ the Fe moments have a random orientation and do not lie in the plane of the substrate. For $CIT_{0.59}$ a small preferred orientation inside the substrate plane can be inferred from the r value of 2.15. This could be an effect due to the cylinder-like structure of $CIT_{0.59}$, the magnetic moments having a slight tendency to align along the

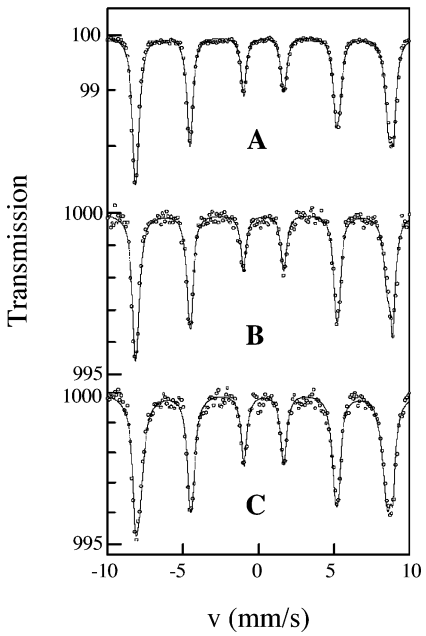

Figure 3. ^{57}Fe Mössbauer absorption spectra at 4.2 K in zero applied field for (A) CIT_0 nanocrystals dispersed in PVA, (B) $CIT_{0.59}$ nanocrystals, and (C) $DO_{0.59}$ nanocrystals.

cylinder axis. However, it can be concluded that the structuring field during the deposition does not significantly orient the easy axes for both coatings (CIT and DO) of the nanocrystals. Hence, the easy axes of the nanocrystals are not perfectly oriented inside the cylinders. We also checked the influence of a small preferential easy axis orientation on the hysteresis loops, to determine whether the hysteresis curve data for the CIT nanocrystals can be accounted for by the slight magnetic texture. The distribution function $f(\theta)$ of the easy axes orientations can be modeled by the probability law:

$$\boldsymbol{P}(\theta) = C \sin\theta \exp\left(-\frac{(\cos\theta - 1)^2}{\sigma^2}\right) \qquad (2)$$

where σ is the orientational degree and θ is the angle between the direction of the structuring field and the magnetic moment, or easy axis. When the angular averages of the line intensities (1) are evaluated with the $f(\theta)$ function, the ratio $r = A_{2,5}/A_{3,4}$ can be linked to the orientational degree σ. Then for a given easy axis distribution, the hysteresis loop in the direction of the measuring field with respect to the film structure is calculated for uniaxial nanocrystals without interactions. Figure 4 shows the hysteresis loops calculated for various r values. The hysteresis loops obtained for $r = 2.15$, corresponding to $CIT_{0.59}$ nanocrystals, and for the random orientation ($r = 2$) are not significantly modified. Therefore, the slight orientation of the easy axes observed above for CIT nanocrystals has no influence on the hysteresis curve. The Mössbauer spectroscopy data are also in agreement with the fact that no preferential crystal alignment along the chain direction is observed by high-resolution TEM images for diluted systems. This can be attributed to the fact that the size polydispersity of the sample as well as the imperfect spherical shape of the nanocrystals induced defects of the nanocrystals packing inside cylinders.

Hence, the change in the magnetic properties with the coating when a magnetic field is applied during the deposition is attributed to the structure induced in the film by the structuring field. In these systems only the dipolar interactions between particles can induce a structure-dependent magnetization curve.

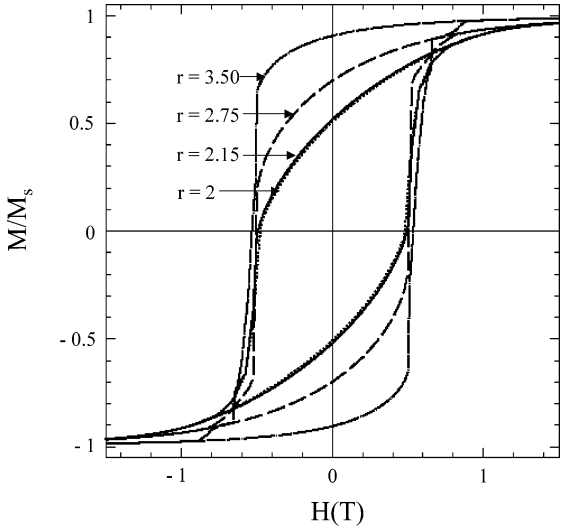

Figure 4. Theoretical hysteresis loops at 0 K for uniaxial particles without interactions, for different degrees of orientation of the easy axes around the structuring field. The curves are labeled according to the value of the Mössbauer line intensity ratio r, which is also a measure of the orientational degree (see text).

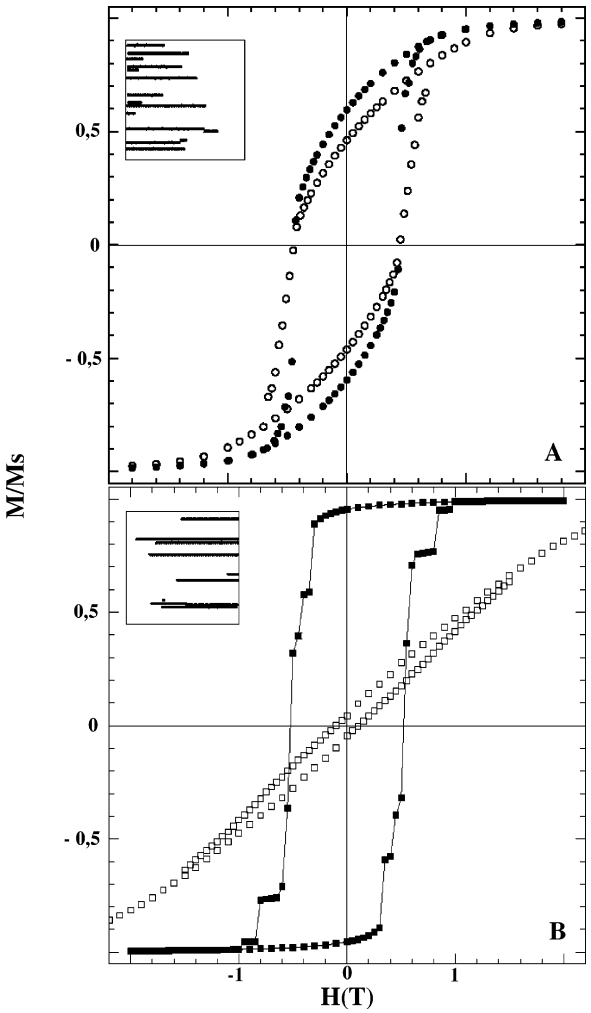

Figure 5. Theoretical magnetization curves for particles in linear chains for (A) $\alpha = 0.04$ and (B) $\alpha = 0.39$. The measuring field is either parallel (solid symbols) or perpendicular (open symbols) to the chains. The inset shows the chainlike structure of the system.

The complete study of the effect of the dipolar interactions on the magnetic properties of such three-dimensional (3D) structures made of spherical nanocrystals is still to be done. However

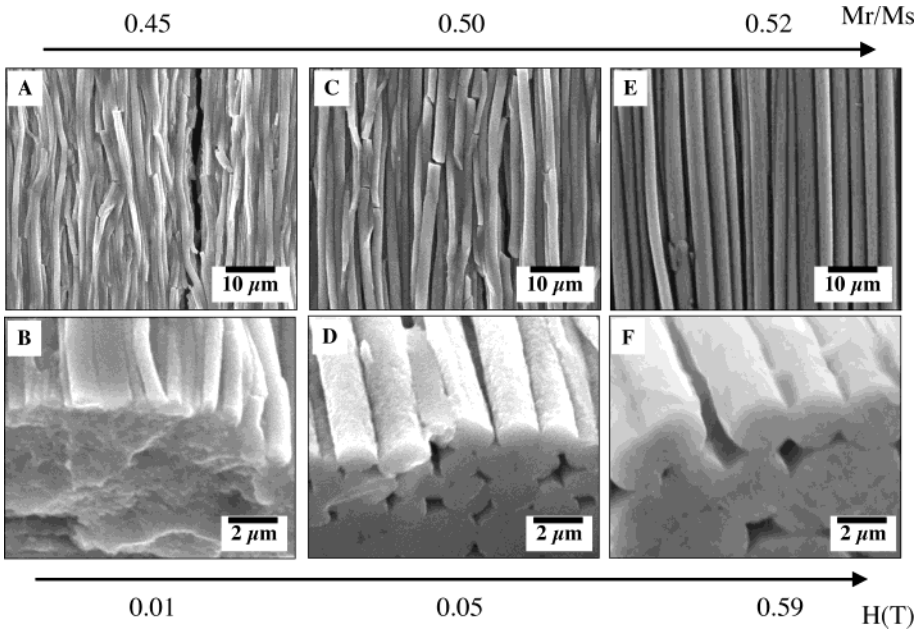

Figure 6. SEM images obtained at various magnifications for maghemite nanocrystals evaporated in various applied magnetic field strengths: (A,B) $CIT_{0.01}$ nanocrystals; (C,D) $CIT_{0.05}$ nanocrystals; (E,F) $CIT_{0.59}$ nanocrystals.

we can make a parallel case with what we already know about two-dimensional (2D) assemblies of spherical magnetic particles.[14] For such systems, the magnetization curves for different kinds of structures have been calculated. It has been shown that the magnetization curve is sensitive to the structure in the layer only when the particles are arranged in linear chains parallel to a given direction, even for randomly distributed easy axes. In these calculations the particles are characterized by their saturation magnetic moment, M_s, their anisotropy constant K, and their diameter D. Then for a well-ordered lattice characterized by a lattice spacing d, one can introduce a coupling constant $\alpha_d = \pi M_s^2/12K(D/d)^3$. When the particles are arranged in chainlike structures, we can define an effective coupling constant, α_d^{eff}, by using the properties of the dipolar interaction, namely, its long range dependence $(1/r^3)$ and its anisotropy. This effective coupling constant defines a reference system, which is a square lattice characterized by a coupling constant $\alpha_d = \alpha_d^{\text{eff}}$. Then, the influence of the structure on the magnetization curve of the actual system shows up through the difference between the magnetization curve of the reference system, $M_{\text{ref}}(H)$, and that of the actual system, $M(H)$. For small values of α_d^{eff}, the organizations of the particles in linear and parallel chains are responsible for a squarer (respectively smoother) hysteresis loop when the measuring field is parallel (respectively perpendicular) to the chain direction. The value of the remanence magnetization is modified, whereas the value of the coercive field remains nearly constant. In our experimental conditions, the estimated average distance between nanocrystals, deduced from the TEM pictures in dilute solution, is $d = 1$ nm, the nanocrystal mean diameter is 10 nm, and the saturated magnetization and the anisotropy constants are 77 emu g^{-1} and 6×10^5 erg cm^{-3}, respectively. This yields $\alpha = 0.04$, corresponding to a low coupling constant. The calculated hysteresis loop for such low coupling (0.04) shows an increase in the reduced remanence and no change in coercivity field (Figure 5A) when going from the parallel to the perpendicular configuration. When the coupling is increased, the coercive field is also changed and the hysteresis loop with the measuring field parallel to the chains encloses that with the field perpendicular to the chains, the loop of the diluted system (i.e., $\alpha_d \rightarrow 0$) lying in between. For a very large coupling (0.39), drastic changes in the hysteresis loop and coercivity are observed (Figure 5B). Thus, for a 2D linear chain orientation, no change is expected in the coercivity by changing the applied field direction in the limit of small coupling. However, we are presently dealing with 3D structures and the parallel with the 2D situation must be done with care, because dipolar systems are a priori strongly influenced by the dimensionality of the whole system as a result of the long range character of the dipolar interaction. Nevertheless, we may conclude that the changes we see in the magnetization curves are really due to the influence of the structuring field on the organization of the film.

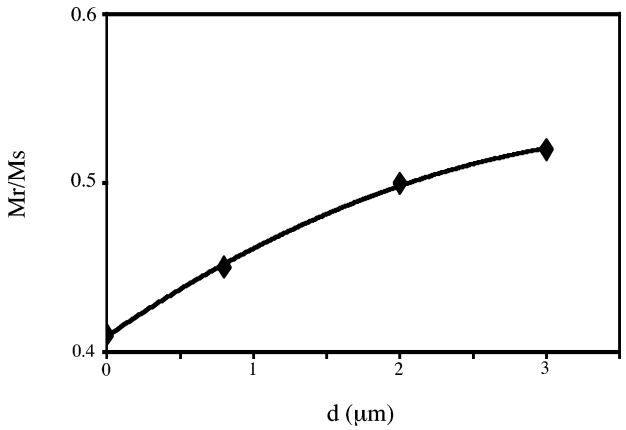

Figure 7. Variation of the reduced remanence with the average width d of the "tubes" obtained for maghemite CIT nanocrystals evaporated under various applied magnetic field strengths: 0.01, 0.05, and 0.59 T.

To confirm such claims, magnetization measurements are compared for a CIT sample submitted to various applied fields, x, during the deposition process. Whatever the strength of the applied field, we find that nanocrystals are aligned along the direction of the magnetic field in tubelike structures. Figure 6 shows that the average width of the "tubes" and their compacity increase in the structuring magnetic field. We also find that, for the parallel geometry $CIT_x(\|)$, the reduced remanence increases with the average width d of the "tubes" (Figure 7),

TABLE 2: Variation of the Reduced Remanence at 3 K, for Particles Coated with Citrate Ions, Deposited in a Magnetic Field of 0.01, 0.05, and 0.59 T during Evaporation[a]

sample:	$CIT_{0.01}(\|\|)$	$CIT_{0.01}(\perp)$	$CIT_{0.05}(\|\|)$	$CIT_{0.05}(\perp)$	$CIT_{0.59}(\|\|)$	$CIT_{0.59}(\perp)$
M_r/M_S:	0.45	0.37	0.50	0.30	0.52	0.31
ΔH_c ($H_c\|\| - H_c\perp$) (Oe):	50		50		90	

[a] For the oriented deposits, the measuring field is applied parallel to the substrate and is either (||) along the direction or (⊥) perpendicular to the aligned particles.

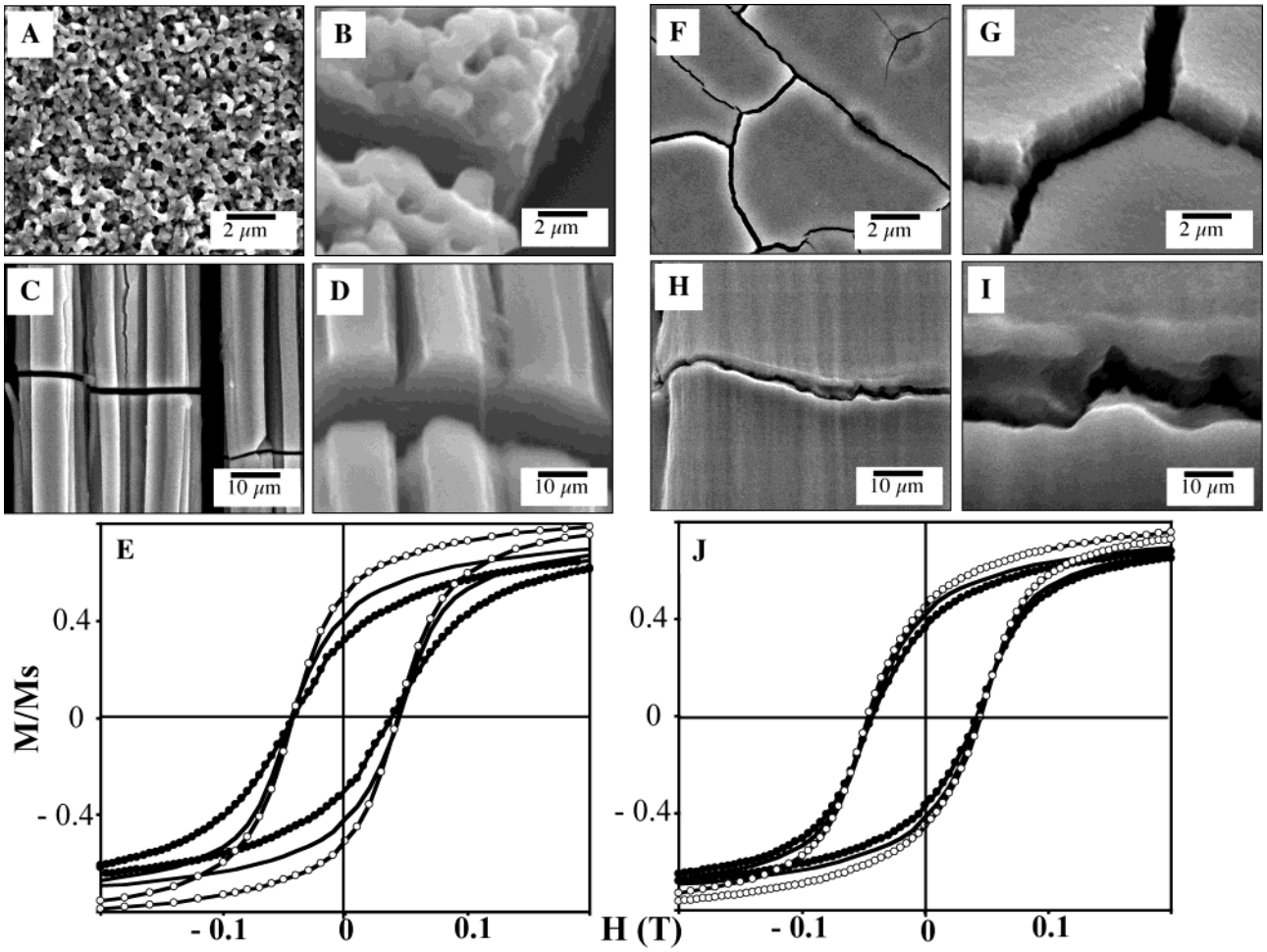

Figure 8. Upper part shows SEM images obtained at various magnifications for maghemite nanocrystals evaporated in the absence and presence of a magnetic field, coated with OC_0 nanocrystals (A,B) and PR_0 nanocrystals (F,G), for $OC_{0.59}$ nanocrystals (C,D), or $PR_{0.59}$ nanocrystals (H,I). Lower part shows magnetization curves at 3 K recorded for OC nanocrystals (E) and PR nanocrystals (J) with either no field (solid line) or a 0.59 T field applied during the deposition (process), the measuring field being along the *x* (○) and *y* (●) direction.

whereas in the perpendicular geometry $CIT_x(\perp)$, it decreases (Table 2). The coercivity field is rather low and the difference in the remanence ratio value when the field is (||) and (⊥) to the orientation of the tubes is not significant and lies within experimental uncertainty. From these data, the emerging picture is that the structuring field, aligning the nanocrystals more or less in chains parallel to its direction, is the key parameter to induce a change in the reduced remanence. The influence of the alignment of the nanocrystals is confirmed by using two other types of coatings: γ-Fe_2O_3nanocrystals coated with octanoic acid (OC) and propanoic acid (PR). OC nanocrystals are solubilized in cyclohexane, whereas PR nanocrystals are dispersed in aqueous solution. The same procedure as described above is used for OC and PR nanocrystals. During the deposition (process) the ferrofluid is or is not subjected to a 0.59 T applied magnetic field. With OC_0 nanocrystals, a thin film made of spherical highly compact agglomerates with a very rough surface (Figure 8A,B) is observed, whereas long cylinders with a very regular structure are formed with $OC_{0.59}$ (Figure 8C,D). The

TABLE 3: Variation of the Reduced Remanence and Coercivity at 3 K for Deposited Particles Differing by Their Coating[a]

sample:	OC_0	$OC_{0.59}(\|\|)$	$OC_{0.59}(\perp)$	PR_0	$PR_{0.59}(\|\|)$	$PR_{0.59}(\perp)$
M_r/M_S:	0.41	0.50	0.32	0.42	0.45	0.36
H_c (Oe):	400	430	380	420	440	400

[a] The measuring field is applied parallel to the substrate and is either (||) along the direction or (⊥) perpendicular to the aligned particles.

SEM patterns obtained with OC are similar to those obtained with CIT nanocrystals (Figure 1A,C,E) dispersed in two solvents (cyclohexane and water respectively). Figure 8E shows that the hysteresis loops of $OC_{0.59}$ (||) and $OC_{0.59}$ (⊥) are similar to those obtained with $CIT_{0.59}$ (||) and $CIT_{0.59}$ (⊥) (Figure 2A). Hence, the magnetic responses obtained with OC_0, $OC_{0.59}(\|\|)$, and $OC_{0.59}(\perp)$ (Table 3) are similar to those obtained with CIT_0, $CIT_{0.59}(\|\|)$, and $CIT_{0.59}(\perp)$ (Table 1). This clearly indicates that a similar magnetic behavior occurs when the nanocrystals are aligned in tubelike structures.

With PR nanocrystals dispersed in aqueous solution, the SEM patterns of PR_0 show formation of a dense thick film (Figure 8F,G). Slight undulations are observed with $PR_{0.59}$ (Figure 8H,I). The hysteresis loop recorded with $PR_{0.59}(\|)$ is slightly squarer than that obtained with PR_0 (Figure 8J). Magnetic responses obtained with PR_0, $PR_{0.59}(\|)$, and $PR_{0.59}(\perp)$ (Table 3) slightly differ from those obtained with DO_0, $DO_{0.59}(\|)$, and $DO_{0.59}(\perp)$ (Table 1). The magnetic behavior observed with PR nanocrystals seems to be intermediate between that obtained with DO at one end and those obtained with CIT and OC at other the end. This could be related to the presence of better-defined stripes with $PR_{0.59}$ (Figure 8H,I) compared to $DO_{0.59}$ (Figure 1D,F). From these data it is concluded that nanocrystals aligned along a given direction behave as nanowires. It seems reasonable to claim that the width of the tubes plays a role in defining the magnetic behavior. However, because two parameters vary simultaneously it is rather difficult to reach a final conclusion. Moreover, because there is a large change in the coercive field, we do not rule out the possibility that the structuring field could lead to an increase in the nanocrystal volume fraction and accordingly to an increase in the effective coupling constant.

IV. Conclusion

It is demonstrated that nanocrystal organizations and magnetic properties differ drastically according to the nanocrystal surface coating. When nanocrystals form tubelike structures, the magnetization behaviors are correlated with the shape anisotropy induced by the organization of the sample.

V. Appendix

Maghemite γ-Fe_2O_3 nanocrystals are prepared by the synthesis described previously,[15] with slight changes. Dimethylamine ($(CH_3)_2NH_2OH$) is added to an aqueous solution of ferrous dodecyl sulfate ($Fe(DS)_2$). The final concentrations after the reactants are mixed are 1.3×10^{-2} mol L^{-1} and 8.5×10^{-1} mol L^{-1} for $Fe(DS)_2$ and dimethylamine, respectively. The solution is then stirred vigorously for 2 h at 28.5 °C. A precipitate appears which is isolated from the supernatant by centrifugation. At this stage uncoated γ-Fe_2O_3 nanocrystals are produced. Two different procedures are used to coat nanocrystals.

(i) The procedure used for coating with citrate ions is as follows: The precipitate is washed with HNO_3 (10^{-2} mol L^{-1}) until a solution at pH 2 is reached. Sodium citrate dissolved in water ($[Na_3C_6O_7H_5] = 1.5 \times 10^{-2}$ mol L^{-1}) is then added to the solution. The mixture is subjected to sonication for 2 h at 90 °C. Acetone addition induces precipitation of the nanocrystals, and after they are washed with a large excess of acetone, the obtained powder, consisting of nanocrystals coated with citrate ions, is dried in air.

(ii) The procedure used for coating with carboxylic acids ($C_nH_{2n+1}COOH$) differing by the alkyl chain length ($n = 2$, $n = 7$, $n = 11$) is as follows: The precipitate of uncoated nanocrystals is washed with a large excess of ethanol. Then a solution of carboxylic acid solubilized in ethanol ($[C_nH_{2n+1}COOH] = 1.4 \times 10^{-1}$ mol L^{-1}) is added. The solution is subjected to sonication for 2 h at 90 °C. A precipitate appears, which is washed with a large excess of ethanol, and the powder is dried in air. The nanocrystals coated with propanoic acid ($n = 2$) are dispersed in water, whereas the nanocrystals coated with octanoic acid ($n = 7$) and dodecanoic acid ($n = 11$) are dispersed in cyclohexane.

All the solutions with their different coatings are kept on a magnet for 12 h in order to discard unstable nanoparticles, and the supernatant is then collected. X-ray diffraction lines indicate an inverted spinel structure for all the coated nanocrystals with a lattice constant of 8.360 Å. Hence, depending on the coating agent, hydrophilic (citrate ions and propanoic acid) and hydrophobic (octanoic and dodecanoic acid) magnetic fluids are obtained.

References and Notes

(1) Martin, J. I.; Nogues, J.; Liu, K.; Schuller, I. K. *J. Magn. Magn. Mater.* **2003**, *256*, 449.
(2) Khan, H. R.; Petrikowski K. *J. Magn. Magn. Mater.* **2000**, *526*, 215−216.
(3) Zheng, M.; Menon, L.; Liu, Y.; Bandyopadhyay, S.; Kirby, R. D.; Sellmyer, D. J.; Ebels, U.; Huynen, I. *Phys. Rev. B* **2000**, *62*, 12282.
(4) Encinas-Oropesa, A.; Demand, M.; Piraux, L. *J. Appl. Phys.* **2001**, *89*, 6704.
(5) Ngo, A. T.; Pileni, M. P. *Adv. Mater.* **2000**, *12*, 276.
(6) Ngo, A. T.; Pileni, M. P. *J. Phys. Chem. B* **2001**, *105*, 53.
(7) Lalatonne, Y.; Richardi, J.; Motte, L.; Pileni M. P.; to be submitted for publication.
(8) Ngo, A. T.; Bonville, P.; Pileni, M. P. *Eur. Phys. J. B* **1999**, *9*, 583.
(9) Stoner, E. C.; Wohlfarth, E. P. *Philos. Trans. R. Soc. London, Ser. A* **1948**, *240*, 559. Reprinted in *IEEE Trans. Magn.* **1991**, *27*, 3475.
(10) Walker, M.; Mayo, P. I.; Grady, K. O.; Charles, S. W.; Chantrell, R. W. *J. Phys.: Condens. Matter.* **1993**, *5*, 2779.
(11) Gazeau, F.; Bacri, J. C.; Gendron, F.; Perzynski, R.; Raikher, Yu. L.; Stepanov, V. I.; Dubois, E. *J. Magn. Magn. Mater.* **1998**, *186*, 175.
(12) Pileni, M. P. *Adv. Funct. Mater.* **2001**, *11*, 323.
(13) Koutani, S.; Gaveille, G.; Gerardin, R. *J. Magn. Magn. Mater.* **1993**, *123*, 175.
(14) Russier, V.; Petit, C.; Pileni, M. P. *J. Appl. Phys.*, in press.
(15) Moumem, N.; Veillet, P.; Pileni, M. P. *J. Magn. Magn. Mater.* **1995**, *149*, 67.